Characterisation and Modelling of Mg Doped ZnO TFTs

A. Shaw, C. Gao, J. D. Jin, I. Z. Mitrovic and S. Hall
Department of Electrical and Electronic Engineering,
University of Liverpool,
Liverpool, UK.

***Abstract* - The ever-increasing use of ZnO TFTs requires further in depth analysis and the need for a suitable model to obtain the true transport mechanisms. This paper explores the modelling of MgZnO TFTs using a defect state model based on multiple trapping and release and successfully validates the model with the fitting parameters. Namely, flat band voltage, characteristic temperature associated with the defect distribution, number of traps and conductivity of the ZnO film.**

Keywords—Zinc oxide (ZnO), Magnesium doped Zinc Oxide (MgZnO), atomic layered deposition (ALD), thin film transistor (TFT), TFT modelling.

I. INTRODUCTION

Zinc Oxide (ZnO) has gathered great interest within the semiconductor industry over the last decade due to its large direct band gap (~3.3 eV), natural *n*-type conductivity and large exciton binding energy (60 meV) [1]. This has led ZnO to being an attractive transparent metal oxide semiconductor for the use in an ever-growing display electronics industry. Currently indium-gallium-zinc-oxide (IGZO) is the leading transparent metal oxide semiconductor which is rivalling a-Si:H in active matrix for large displays [2]. However, indium is a rare and expensive element which can suffer from large fluctuations in price reducing the attractiveness of IGZO as a long term, high performing semiconductor material for displays application.

Previous reports have demonstrated that ZnO based TFTs have higher operational speeds than IGZO TFTs [3]. The films are typically < 50 nm and different deposition techniques such as RF sputtering [4], sol-gel [5] and atomic layer deposition (ALD) [6] are employed. The intrinsic conductivity of the films is related to defects, most notably interstitials (Zn_i) and oxygen vacancies (V_o) [1]. In this paper we further explore our published work on magnesium (Mg) doping using ALD in order to reduce the number of Zn_i and V_o defects [7]. Furthermore, the incorporation of Mg in ZnO films is seen to increase the band gap of ZnO, thus increasing the optical transparency of the films presumably due to the presence of magnesium oxide (MgO) which has a band gap of 7.7 eV [8].

Moreover, for ZnO TFT data extraction, the standard method adopted in most literature, is to use the standard crystalline Si MOSFET equations. However, it is evident that TFTs do not follow an exponential and square law delineated by a well-defined threshold voltage, but rather a generic power law over the entire range of current. The simplistic analysis does not explain the true transport mechanism within the ZnO films. Currently, only a few models have been proposed based on either poly-Si or amorphous Si (a-Si:H SPICE) related to the presence of grain boundaries and defect state distribution. The SPICE based model by Iniguez et al. [9] successfully fitted ZnO TFTs but there is no explanation of underlying transport mechanisms. The model requires many empirical fitting parameters. The grain boundary model of Hossain et al. [10] explains a possible transport mechanism within the film, but does not fit the model to any experimental data. The defect state distribution model of Torricelli et al. [11] uses the well-known multi-trapping and release model [12] to explain the transport of electrons within the tail state traps which originate near to the conduction band edge. These traps arise from defects associated with the polycrystalline/amorphous nature of ZnO films. The advantages of this model are that the fitting parameters are physical attributes of semiconductors and can be extracted from experimental data. The model reduces to the standard crystalline Si MOSFET equations, under appropriate conditions. In this work, the MTR model is applied to fit Mg doped TFT experimental data. Furthermore, the influence of Mg doping on the ZnO bandgap is reported.

II. FABRICATION

Mg doped ZnO (MgZnO) layers were deposited using ALD at 200 ^oC to a thickness of 50 nm. The precursors used were H_2O, Diethylzinc and Bis(ethylcyclopentadie-nyl)magnesium (Mg), where the cycle ratio between the Zn and Mg precursors was varied to alter the Mg composition. The selected ratio for this paper was 7:1 of Zn:Mg. All of the MgZnO were grown on substrate that consisted of n^+-Si and 50 nm thermally grown SiO_2. For the TFT fabrication, the standard photolithography and lift-off processes were used to pattern the source and drain contacts. For the contacts, Al was evaporated to a thickness of 80 nm. The TFTs were then isolated using a wet etching process. All the TFTs were subjected to annealing at 300 ^oC in air for 1 hour post fabrication. The TFT structure used throughout this paper is shown in Fig. 1.

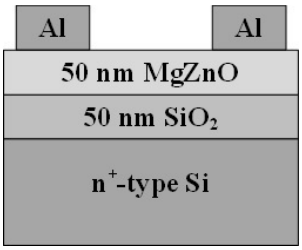

Fig. 1: Cross section of the bottom gate and top contact MgZnO TFT

III. Results And Discussion

Before the TFTs were fabricated, the thickness and band gap of the MgZnO were measured with a J.A. Woollam M2000 spectral ellipsometer at the three angles 65^0, 70^0 and 75^0. The fitting was performed using WVASE software with the predefined ZnO model used from the library. A film thickness of ~50 nm was obtained by fitting in the transparent region of the spectrum. The direct band gap approximation Tauc plot is shown in Fig. 2 where it can be seen that the band gap (E_g) has increased from 3.28 eV to 3.47 eV for the MgZnO. This increase in band gap is comparable with other reported ALD grown MgZnO with cycle ratios of 7:1 [7,13].

The TFT transfer and output characteristics for n^+-Si substrates were measured and shown in Figs. 3(a) and (b) respectively. To benchmark the performance of the TFTs with published reports, the effective saturation mobility (μ_{sat}) and threshold voltage (V_T) were extracted assuming the standard MOSFET equation

$$I_D = \frac{W}{2L}\mu_{sat}C_{ox}(V_{GS}-V_T)^2 \qquad (1)$$

where W and L are the channel width and length respectively, C_{ox} the gate oxide capacitance per unit area and V_{GS} the gate source voltage. The effective subthreshold swing (SS) was also extracted at the steepest part of the transfer slope using the following equation

$$SS = \left(\frac{d\log(I_D)}{dV_{GS}}\right)^{-1} \qquad (2)$$

Note that (2) also implies a standard Si model for the low current regime. The on/off ratio ~$7\text{x}10^6$, where V_{on}=-0.5 V and is the voltage required to establish a significant conducting channel [8]. Furthermore, μ_{sat}= 3.6 cm^2/Vs, V_T=8.14 V and SS= 0.84 V/dec. Table 1 shows a comparison of our TFT with published ALD grown ZnO TFTs. The performance of our TFT is comparable with [14] and [16], where the gate oxide used was also SiO_2.

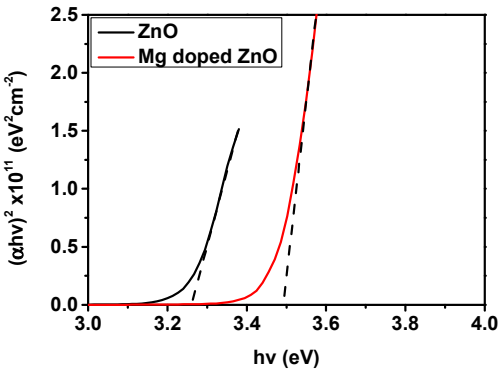

Fig. 2: Tauc plot for ZnO and MgZnO deposited at 200 ^{0}C where α is the absorption coefficient and $h\upsilon$ is the photon energy.

TABLE I. COMPARISON OF TFT PERFORMANCE USING THE STANDARD MOSFET EQUATION.

Device	W/L (μm/μm)	On/Off	μ_{sat} (cm^2/Vs)	V_T (V)	SS (V/dec)
This work	400/40	$7.2\text{x}10^6$	3.6	8.14	0.84
[14]	100/10	$8\text{x}10^6$	0.9	N/a	2.26
[15]	40/20	$9.46\text{x}10^7$	6.7	4.1	0.67
[16]	1600/200	$2.43\text{x}10^6$	0.13	13.1	1.21

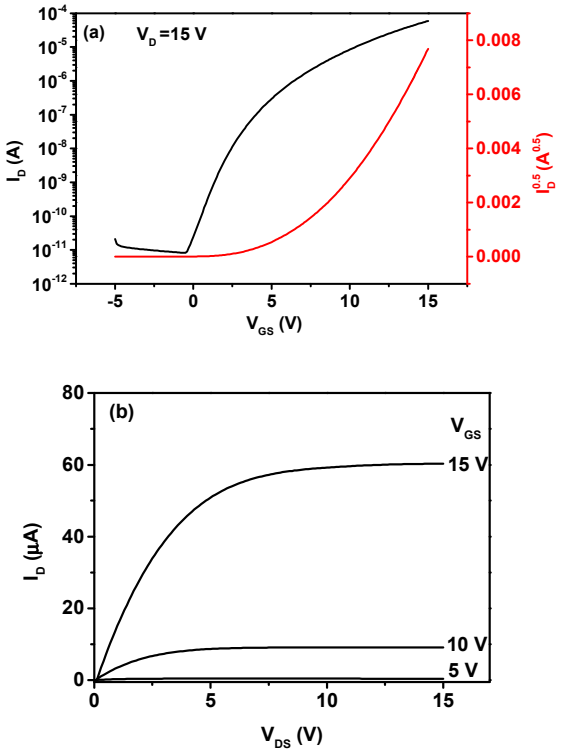

Fig. 3: (a) Transfer characteristic and $I_D^{0.5}$-V_{GS} where V_{DS}=15 V and (b) Output characteristic of the MgZnO.

It is evident from Fig. 3(a) that the transfer curve does not follow a square law but rather a power law. We adopt the model proposed by Torricelli et al. [9] with the following equation to express the drain current

$$I_D = \frac{W}{L}\beta\left[(V_{GS}-V_{FB}-\varphi_S)^\gamma-(V_{GS}-V_{FB}-\varphi_D)^\gamma\right] \qquad (3)$$

where V_{FB} is the flat band voltage, φ_S and φ_D the surface potentials at the source and drain, $\gamma=2T_o/T$ where T is the temperature, T_o is the characteristic temperature associated with the exponential trap distribution and β is defined as

$$\beta = \sigma_o\frac{\varepsilon_s}{C_{ox}}V_t\left(\frac{1}{\gamma-1}\right)\left(\frac{C_{ox}^2\sin\left(2\pi/\gamma\right)}{2\pi N_t q\varepsilon_s V_t}\right) \qquad (4)$$

where σ_o is a conductivity pre-factor, ε_s is the permittivity of ZnO, N_t is the number of traps, q is the charge of an electron, and V_t is the thermal voltage (kT/q). The surface potentials φ_S are now defined as the source voltage and φ_D as the drain voltage in the triode region and V_{GS}-V_{FB} in the saturation region.

The fitting to the experimental data in Fig. 3(a) was applied using (3) and (4) and a linear regression methodology with four fitting parameters; V_{FB}, T_o, σ_o and N_t. Figs. 4(a) shows an excellent fit of the experimental data beyond V_{on}, with a mean squared error (MSE) of 0.16. The fitting parameters extracted are V_{FB} = -0.34 V, T_o = 737 K, N_t = 2.04x10^{19} cm^{-2} and σ_o=7.08 S/cm. The values are realistic for this material, although it is recognised that there is always uncertainty in such a fitting procedure. Further work is underway to measure each parameter independently. It is worth mentioning that a value of T_o= 737 K corresponds to a Meyer-Neldel energy of ~63 meV implying a high degree of disorder in the films. Fig. 4(b) shows the output fitting where the MSE=0.16, 0.04 and 0.13 and when V_{GS}=5, 10 and 15 V respectively.

In order to further fit the output characteristics, it was necessary to modify equation (3) to include the source and drain series resistances R_S and R_D

$$I_D = \frac{W}{L}\beta\left[(V_{GS} - V_{FB} - \varphi_s - (I_D R_S)^{\gamma} - (V_{GS} - V_{FB} - \varphi_D - (I_D R_D)^{\gamma}\right] \quad (5)$$

Fitting with the modified equation, Figs. 5(a) and (b) show the transfer and output characteristic fittings with R_{DS} respectively where V_{FB}=−0.34 V, T_o=752 K, N_t=2.18x10^{19} cm^{-2}, σ_o=8.1 S/cm and R_S=R_D=752 Ω. The transfer characteristic was fitted to an accuracy of MSE=0.07 and the output characteristic to MSE=0.26, 0.09 and 0.1 when V_{GS}= 5, 10 and 15 V respectively. With the low MSE values for both, transfer and output characteristics, the model parameters have been validated. There is slight variation in T_o, N_t and σ_o between the two models from (3) and (5), where the best fittings include R_{DS}.

To validate the fitting parameter V_{FB}, it can be calculated using the following equation

$$V_{FB} = \Phi_M - \left(\chi - \frac{E_g}{2} - \phi_F\right) \quad (6)$$

where Φ_M is the metal work function, χ is the electron affinity of MgZnO and ϕ_F the Fermi level, assumed to be at the conduction band edge in the heavily doped substrate. Using n$^+$-Si as a gate Φ_M= 4.05 eV, χ_{ZNO}=4.5 eV [17] and E_g=3.5 eV, therefore ideal V_{FB}= −2.2V. However, this model requires V_{FB}=-0.34 V, therefore, ΔV_{FB}=1.86 V (model minus ideal). This discrepancy could be explained by the presence of fixed charge (N_f) within the gate oxide. An estimation for N_f can then be obtained from the following equation

$$V_{FB} = \Phi_M - \left(\chi - \frac{E_g}{2} - \phi_F\right) - \frac{qN_f}{C_{ox}} \quad (7)$$

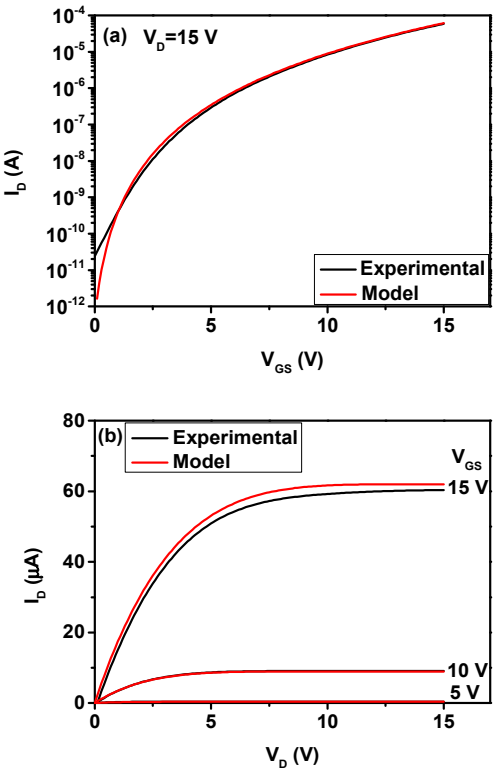

Fig. 4: (a) Transfer characteristic and (b) Output characteristic fitting of the MgZnO TFT with no R_{DS}.

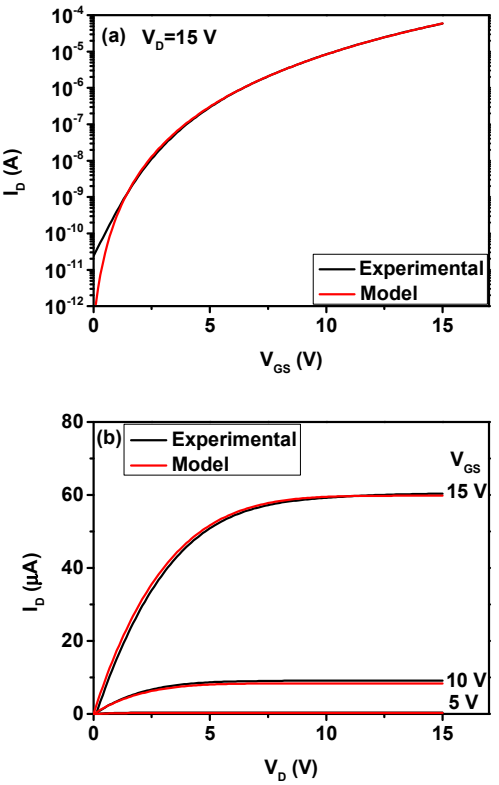

Fig 5: (a) Transfer characteristic and (b) Output characteristic fitting of the MgZnO TFT with R_{DS}.

A value of $N_f \sim -8x10^{11}$ cm^{-2} is extracted from (7). The nature of this negative charge may be related to a large presence of acceptor-like interface states between the SiO_2 and MgZnO and forms the subject of future work.

IV. Conclusion

Accurate TFT modelling has been implemented using a defect state model, where tail states and charge hopping are dominant in the transport mechanism. The fitting parameter V_{FB} correlates with the V_{on} of the TFT, where this parameter is influenced by the fixed charge within the gate oxide. Furthermore, it has been shown that the band gap of MgZnO has increased by ~0.2 eV compared to ZnO, which correlates with other published work.

Acknowledgments

The work has been funded by EPSRC, UK, under project EP/K018884/1. The authors thank J. Wrench and P. Chalker for the ALD research and provision of the MgZnO layers.

References

[1] U. Ozgur *et al.* "A comprehensive review of ZnO materials and devices," J. Appl. Phys., vol. 98, 2005.

[2] Chih-Lung Lin, Wen-Yen Chang and Chia-Che Hung, "Compensating Pixel Circuit Driving AMOLED Display With a-IGZO TFTs," IEEE Electron Device Lett., vol. 34, pp. 1166-1168, 2013.

[3] E. Fortunato, P. Baraquinha and R. Martins, "Oxide Semiconductor Thin-Film Transistors: A Review of Recent Advances". Adv. Mater., vol. 24(22), pp. 2945-2986, 2012.

[4] S. Lee *et al*., "Low-Temperature ZnO TFTs Fabricated by Reactive Sputtering of Metallic Zinc Target". IEEE Trans. Electron Dev. 59 (9), pp. 2555-2558. 2012

[5] Y. H. Hwang, S-J. Seo, B-S. Bae,. "Fabrication and characterization of sol-gel-derived zinc oxide thin-film transistor". J. Mater. Res. 25 (4), pp. 695-700. 2010

[6] B-Y. Oh *et al.*, "High-performance ZnO thin-film transistor fabrication by atomic layered deposition", Semicond. Sci. Technol. 26, 2010.

[7] J. S. Wrench *et al.*, "Compositional tuning of atomic layer deposited MgZnO for thin film transistors". Appl. Phys. Lett. 105(20), pp. 202109. 2014.

[8] R. L. Hoffman, C. Jagadish and S. Pearton, Eds., "Chapter 12 - ZnO thin-film transistors," Zinc Oxide Bulk, Thin Films and Nanostructures, Oxford: Elsevier Science Ltd, 2006, pp. 415-442.

[9] B. Iñiguez *et al.*, "Universal compact model for long- and short-channel Thin-Film Transistors," Solid-State Electron, vol. 52, pp. 400-405, 2008.

[10] F. M. Hossain *et al.*, "Modeling and simulation of polycrystalline ZnO thin-film transistors," J. Appl. Phys., vol. 94, pp. 7768-7777, 2003.

[11] F. Torricelli *et al.*, "Transport physics and device modeling of zinc oxide thin-film transistors part I: Long-channel devices," IEEE Trans. Electron Devices, vol. 58, pp. 2610-2619, 2011.

[12] B. Movaghar, M. Grunewald, B. Pohlmann, D. Wurtz and W. Schirmacher, "Theory of hopping and multiple-trapping transport in disordered systems," J. Stat. Phys., vol. 30, pp. 315-334, 02/01, 1983.

[13] J. C. Armstrong, J. B. Cui and T. P. Chen, "ALD processed MgZnO buffer layers for cu(in,ga)S2 solar cells," in 2014 IEEE 40th Photovoltaic Specialist Conference, PVSC 2014, 2014, pp. 304-307.

[14] J. Yang, J. K. Park, S. Kim, W. Choi, S. Lee and H. Kim, "Atomic-layer-deposited ZnO thin-film transistors with various gate dielectrics," Physica Status Solidi (A), vol. 209, pp. 2087-2090, 2012.

[15] S. J. Lim, S. Kwon, H. Kim and J. Park, "High performance thin film transistor with low temperature atomic layer deposition nitrogen-doped ZnO," Appl. Phys. Lett., vol. 91, 2007.

[16] S. Kwon *et al.,* "Characteristics of the ZnO thin film transistor by atomic layer deposition at various temperatures," Semicond. Sci. and Tech., vol. 24, pp. 035015, 2009.

[17] K. Jacobi, G. Zwicker and A. Gutmann, "Work function, electron affinity and band bending of zinc oxide surfaces," Surf. Sci., vol. 141, pp. 109-125, 6/1, 1984.